

Article

Using Plane Strain Compression Test to Evaluate the Mechanical Behavior of Magnesium Processed by HPT

Amanda P. Carvalho ¹, Leonardo M. Reis ^{2,3}, Ravel P. R. P. Pinheiro ⁴, Pedro Henrique R. Pereira ⁴, Terence G. Langdon ⁵  and Roberto B. Figueiredo ^{4,*}

¹ Department of Mechanical Engineering, Universidade Federal de Minas Gerais, Av. Antônio Carlos 6627, Belo Horizonte 30270-901, MG, Brazil; amandapc@ufmg.br

² Department of Materials Engineering and Civil Construction, Universidade Federal de Minas Gerais, Av. Antônio Carlos 6627, Belo Horizonte 30270-901, MG, Brazil; leomayer@ufmg.br

³ Graduate Program in Metallurgical, Materials and Mining Engineering, Universidade Federal de Minas Gerais, Av. Antônio Carlos 6627, Belo Horizonte 30270-901, MG, Brazil

⁴ Department of Metallurgical and Materials Engineering, Universidade Federal de Minas Gerais, Av. Antônio Carlos 6627, Belo Horizonte 30270-901, MG, Brazil; ravelpimenta@ufmg.br (R.P.R.P.P.); ppereira@demet.ufmg.br (P.H.R.P.)

⁵ Materials Research Group, Department of Mechanical Engineering, University of Southampton, Southampton SO17 1BJ, UK; T.G.Langdon@soton.ac.uk

* Correspondence: figueiredo@demet.ufmg.br; Tel.: +55-3134091925

Abstract: There is a great interest in improving mechanical testing of small samples produced in the laboratory. Plane strain compression is an effective test in which the workpiece is a thin sheet. This provides great potential for testing samples produced by high-pressure torsion. Thus, a custom tool was designed with the aim to test 10 mm diameter discs processed by this technique. Finite element analysis is used to evaluate the deformation zone, stress and strain distribution, and the accuracy in the estimation of stress–strain curves. Pure magnesium and a magnesium alloy processed by high-pressure torsion are tested using this custom-made tool. The trends observed in strength and ductility agree with trends reported in the literature for these materials.

Keywords: magnesium; severe plastic deformation; mechanical properties; mechanical testing; finite element modeling



Citation: Carvalho, A.P.; Reis, L.M.; Pinheiro, R.P.R.P.; Pereira, P.H.R.; Langdon, T.G.; Figueiredo, R.B. Using Plane Strain Compression Test to Evaluate the Mechanical Behavior of Magnesium Processed by HPT. *Metals* **2022**, *12*, 125. <https://doi.org/10.3390/met12010125>

Academic Editors: Andriy Ostapovets and Marcello Cabibbo

Received: 16 December 2021

Accepted: 6 January 2022

Published: 9 January 2022

Publisher's Note: MDPI stays neutral with regard to jurisdictional claims in published maps and institutional affiliations.



Copyright: © 2022 by the authors. Licensee MDPI, Basel, Switzerland. This article is an open access article distributed under the terms and conditions of the Creative Commons Attribution (CC BY) license (<https://creativecommons.org/licenses/by/4.0/>).

1. Introduction

The evaluation of the mechanical behavior in materials produced using laboratory-scale processing techniques is not straightforward. In many cases the samples display small volume and small dimensions preventing fabrication of specimens for conventional mechanical testing. The mechanical properties are then estimated using hardness testing or miniature specimens. This is the case in most samples processed by high-pressure torsion (HPT) for example. High-pressure torsion is a severe plastic deformation technique in which samples in the shape of discs are subjected to torsion under significant pressures [1]. In order to generate the large hydrostatic pressures in the range of a few GPa using laboratory-scale equipment, the sample diameters are usually limited to ~10 mm. Moreover, the thickness of the discs is limited by their diameter since a large diameter-to-thickness ratio must be maintained in order to avoid deformation heterogeneity [2–4]. In practice the processed discs are usually thinner than 1 mm.

The mechanical properties in materials processed by HPT are then estimated using microhardness tests or miniature tensile tests but these tests display significant limitations. Microhardness tests only provide an estimate of the mechanical strength and do not allow evaluation of the stress–strain behavior or strain rate sensitivity. Miniature tensile tests bring technical challenges to cut samples, which usually display cross-sections of less than 1 mm² and it is difficult to perform the tests in conventional equipment. The reduced

specimen length prevents the use of an electronic extensometer reducing the accuracy of strain measurements and the reduced cross-section leads to very small loads during tests requiring the use of special load cells. In spite of the technical challenges it is possible to perform tensile tests with miniature samples using special procedures [5].

Another limitation for mechanical testing of materials processed by HPT is the usual lack of uniform elongation in tension. The materials subjected to severe plastic deformations can reach a condition in which the rate of generation of defects is similar to the rate of recovery, and deformation takes place with negligible hardening [6]. Tensile specimens usually develop necking immediately after yielding and therefore it is not possible to estimate true stress and true strain data for a range of strain. The testing of magnesium alloys processed by HPT is an even harder task because these materials usually display brittle behavior and fracture can occur before any noticeable plastic deformation [7,8]. It is therefore desirable to develop appropriate mechanical testing for these materials and these conditions.

Plane strain compression (PSC) testing, which was developed to study deformation of metals by cold rolling [9], displays many advantages for this situation. The load bearing area does not change during deformation, reducing the tendency for strain localization and allowing the estimation of flow stress for a range of deformation. Most of the specimen is deformed under compressive hydrostatic stress which reduces the tendency for cracking and the samples are usually in the shape of thin sheets. In fact, PSC has been used to investigate the mechanical behavior of pure aluminum processed by accumulative roll bonding [10] which is also a severe plastic deformation technique and also produces thin samples. Thus, the present paper aims to investigate the use of a specially designed PSC tool to test samples of pure magnesium and a magnesium alloy processed by HPT. Finite element modeling (FEM) is used to evaluate the deformation zone and stress state.

2. Procedure

2.1. Design of the PSC Tool

The plane strain compression (PSC) test is rather accurate provided some relations between sample and tool geometry are considered and friction effects are minimized. The most important parameters are the sample width, w , and thickness, t , and the tool breadth, b , which are illustrated in Figure 1a. In order to develop near plain strain conditions, it is important to maintain a ratio of $w/b > 5$. The ratio between the tool breadth and the sample thickness affects the deformation zone shape. It has been shown that there is a good correlation between the pressure and the flow stress for conditions in which $b/t \geq 2$ [11].

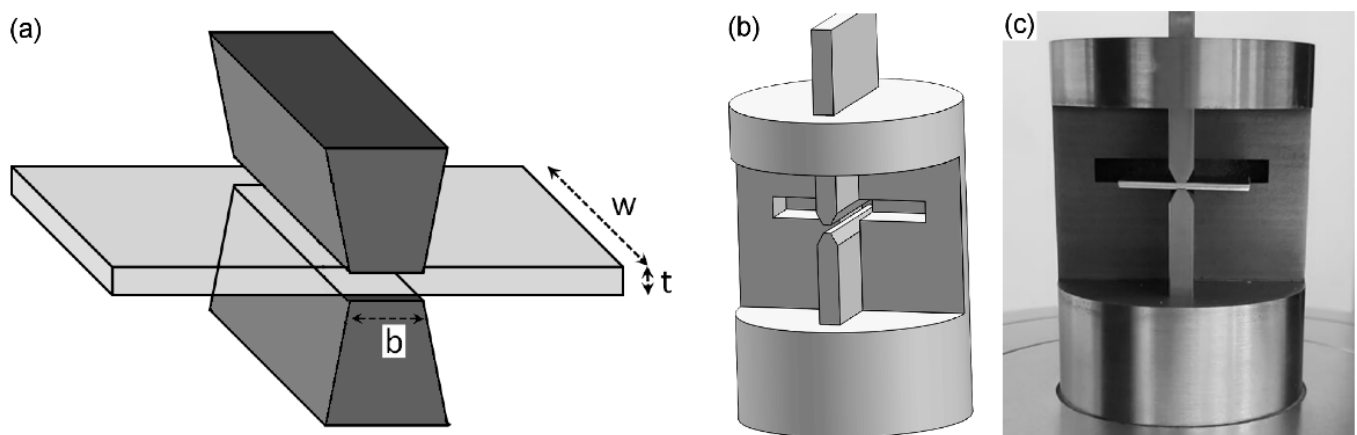


Figure 1. (a) Illustration of the sample and tool parameters, (b) design and (c) photo of a tool for plane strain compression test.

A PSC tool was designed considering these geometric relations and the dimensions of samples produced by HPT processing. The typical dimensions of HPT discs are diameter of ~8 mm or ~10 mm and thicknesses of ~0.7~0.8 mm. An example of the geometry of samples produced by HPT is provided in the following section. Thus, a tool was designed and machined with a breadth of 1.4 mm which allowed the testing of samples with thickness of 0.7 mm or lower and width of 7 mm or larger. An illustration of the tool design and a photo of the PSC apparatus are shown in Figure 1b,c respectively.

2.2. Finite Element Modeling

Finite element modeling of the plane strain compression test was carried out using QForm software (version 10.1.3, QForm Group, Moscow, Russia) [12] considering elasto-plastic conditions. The simulations considered two-dimensional plane strain conditions and also three-dimensional conditions. Figure 2 shows the geometry and mesh for the simulations in (a) 2D and (b) 3D conditions which considered a tool breadth of 1.4 mm, a workpiece thickness of 0.7 mm and a width of 10 mm. Rigid tools were considered in the simulations. The mesh was refined around the deformation area and automatic re-meshing was adopted to avoid significant distortion of the elements. Two friction conditions between the tool and the sample were considered including a frictionless condition and a friction coefficient of 0.15 (Levanov friction condition). The plastic behavior of the sample was modeled considering isotropic behavior and a relationship between effective flow stress, σ , and effective strain, ϵ , is given by Equation (1). The workpiece strain-rate sensitivity was not considered in the simulations.

$$\sigma = 200 \text{ MPa} \times \epsilon^{0.14} \quad (1)$$

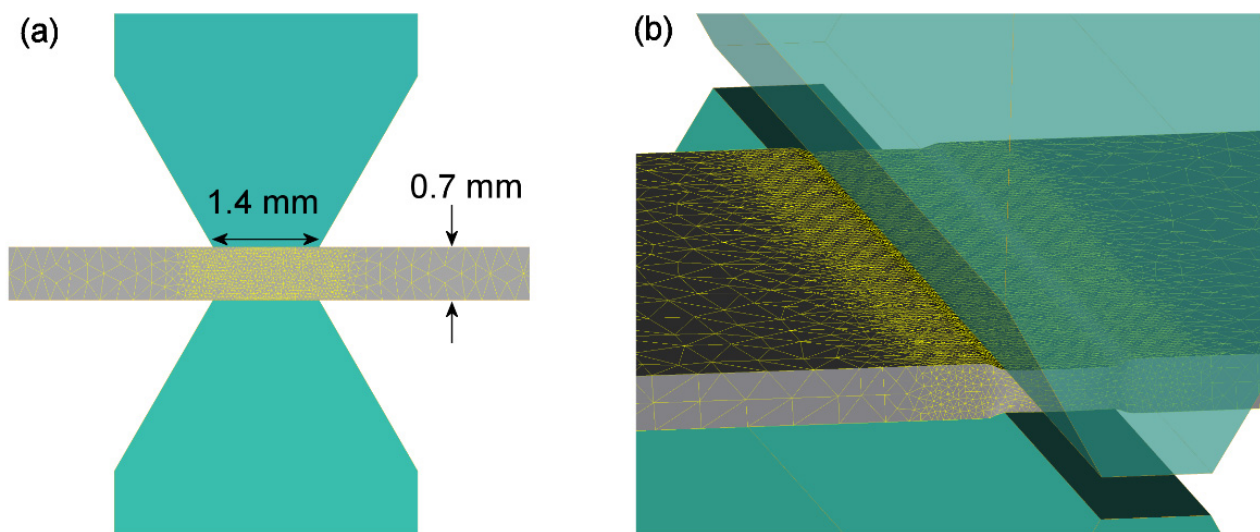


Figure 2. Geometry of tool and sample and mesh details in simulations considering (a) 2D and (b) 3D conditions.

2.3. Experimental Tests in Magnesium

Commercial purity magnesium (hot rolled) and a magnesium alloy AZ31 (Mg-3% Al-1% Zn) (extruded) were used in the present investigation. Samples in the shape of discs with 10 mm diameter and 0.8 mm thickness of both materials were processed by HPT at room temperature under a nominal pressure of 3.8 GPa and a rotation rate of 1 rpm. Processing was carried out using a quasi-constrained facility [13,14] in which the anvils had shallow depressions of 0.25 mm depth and 10 mm diameter. After processing, both surfaces of the discs were ground to a thickness of ~0.7 mm. Care was taken to produce parallel surfaces. Moreover, the edges of the discs were ground to produce parallel lateral surfaces with a width of 7 mm. Figure 3 illustrates the shape of the specimens used for

plane strain compression tests. The areas used in the experiments are highlighted with a different shade. It is observed that the load bearing areas are located apart from the center of the disc. Tests were also carried out in the initial condition of the material for comparison. The hot-rolled pure magnesium was compressed along the through-thickness direction and the extruded AZ31 alloy was compressed along the extrusion direction.

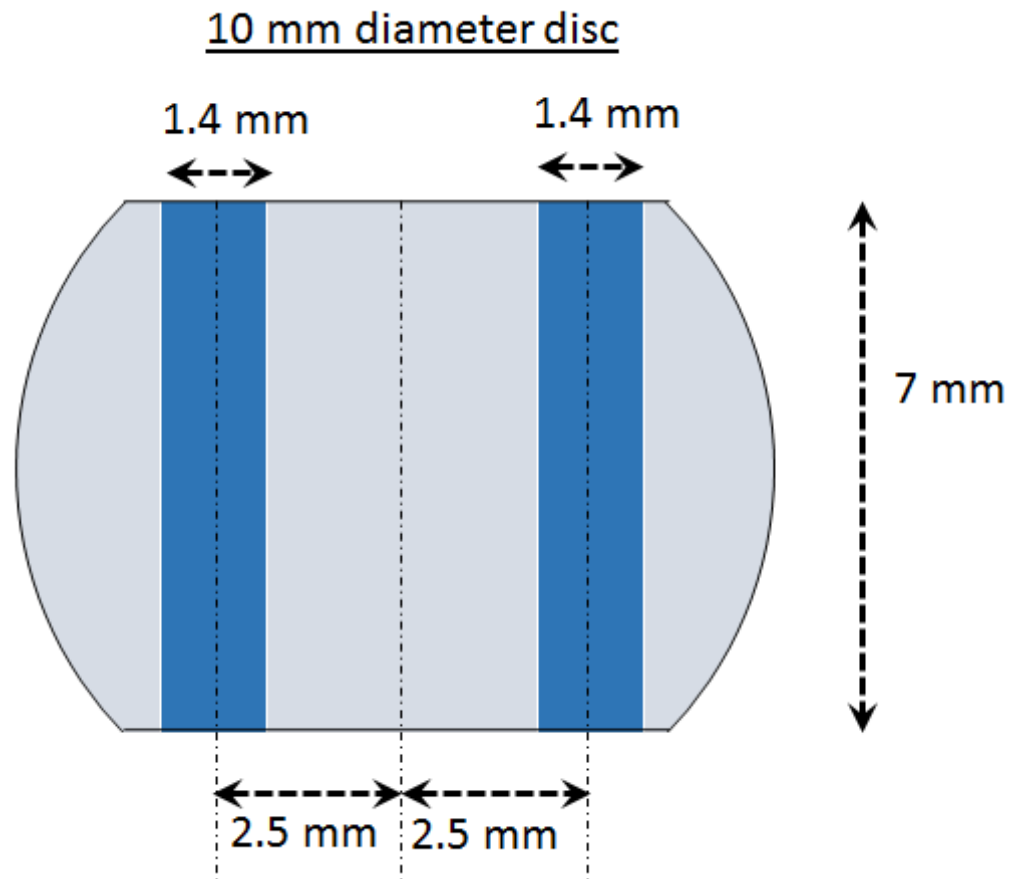


Figure 3. Illustration of the geometry of the specimens prepared from HPT-processed discs and location of the PSC tests.

The plane strain compression tests were carried out at a constant rate of cross-head displacement. The load, P , and displacement, Δt , data were converted to effective stress, σ , and effective strain, ε , [15] using the relationships in Equations (2) and (3) [10,16].

$$\sigma = \sqrt{3}P/2A \quad (2)$$

$$\varepsilon = 2/\sqrt{3} \ln \left(\frac{t_0}{(t_0 - \Delta t)} \right) \quad (3)$$

where A is the load bearing area ($A = 1.4 \text{ mm} \times 7.0 \text{ mm}$) and t_0 is the initial thickness of the specimens ($t_0 = 0.7 \text{ mm}$). In order to determine the contribution from the elastic distortion of the machine and the tool, the system was loaded without any specimen and the relationship between load and elastic displacement was determined. These values were subtracted from the tests with real specimens.

3. Results

3.1. Finite Element Modeling

Figure 4 shows the distribution of (a) strain-rate, (b) plastic strain, and (c) mean stress at different stages of plane strain compression considering 2D condition. The distribution of strain-rate describes the shape of the deformation zone and it is seen that it is not

homogeneous and varies depending on the thickness of the workpiece. Thus, for a thickness of ~ 0.63 mm the deformation zone displays a double “X” shape and it changes to a triple “X” shape at a thickness of ~ 0.47 mm and to a “W” shape at ~ 0.32 mm. This change in the shape of the deformation zone is related to the ratio between the tool breadth and the workpiece thickness. It is worth noting that strain localization in shear bands have been reported in a 5182 aluminum alloy subjected to PSC and the shape of the shear bands varied depending on the sample thickness [17].

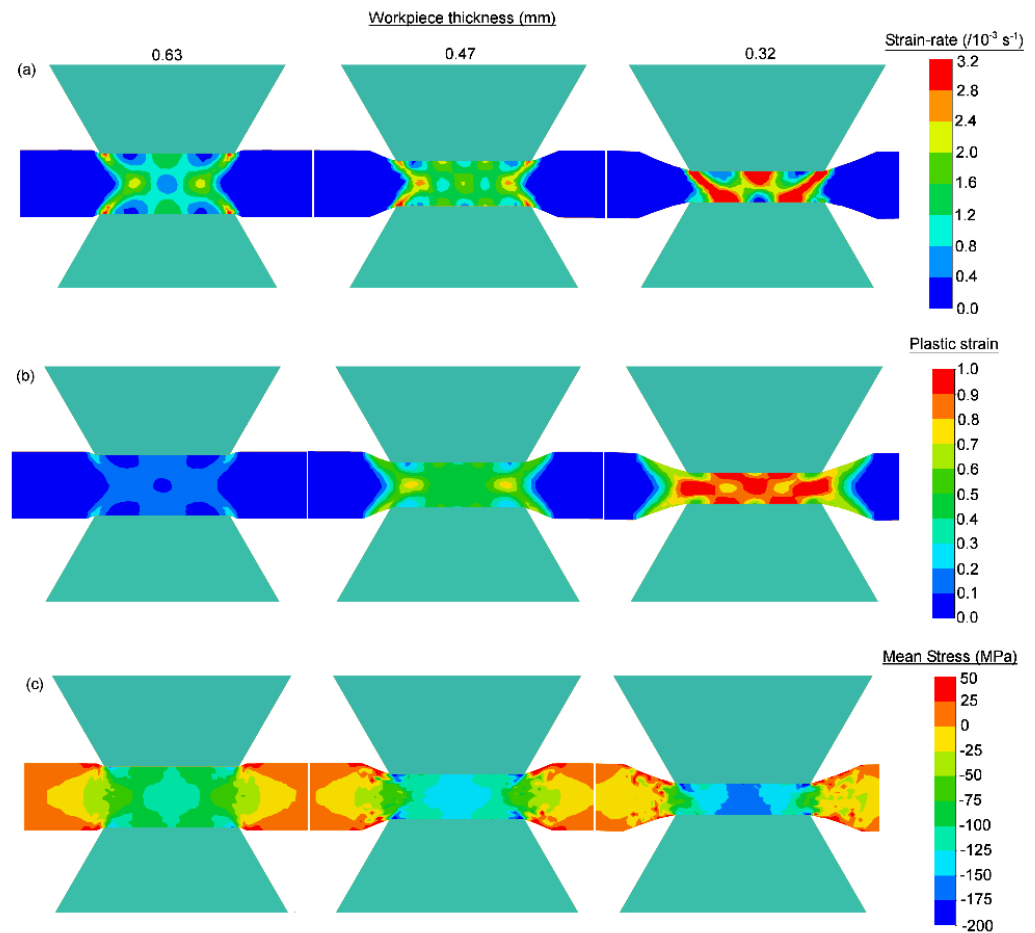


Figure 4. Distribution of (a) strain-rate, (b) plastic strain, and (c) mean stress at different stages of plane strain compression considering 2D conditions.

The heterogeneity of the deformation zone affects the accumulated distribution of plastic strain which is also heterogeneous. For instance, at a thickness of ~ 0.32 mm the effective strain calculated from Equation (3) is ~ 0.90 but values in the range $0.7\sim 1.0$ are observed. The distribution of mean stresses reveal that the deformation zone is located under compressive (negative) mean stresses at all stages of deformation. Tensile stresses develop outside the deformation zone.

Figure 5 shows the distribution of (a) strain-rate, (b) plastic strain, and (c) mean stress at different stages of plane strain compression considering 3D conditions. The results agree fairly well with the simulations considering 2D conditions. The deformation zone displays different shapes including a double “X” shape and a “V” shape for workpiece thicknesses of $0.58\sim 0.66$ mm. These values of thickness provide b/t ratios in the range $2.1\sim 2.4$. The distribution of plastic strain is heterogeneous and values in the range $0.15\sim 0.28$ are observed in a condition in which the nominal strain is ~ 0.22 . Higher values of strain are observed in the workpiece area near the corner of the tool which agrees with previous analysis of this process [18]. The main difference between the 2D and the 3D simulations is

the distribution of mean stresses. The 3D simulation shows that the mean stresses increase near the free surfaces. Most of the sample is deformed under compressive mean stresses though and positive stresses are only observed in a very thin area at the surface.

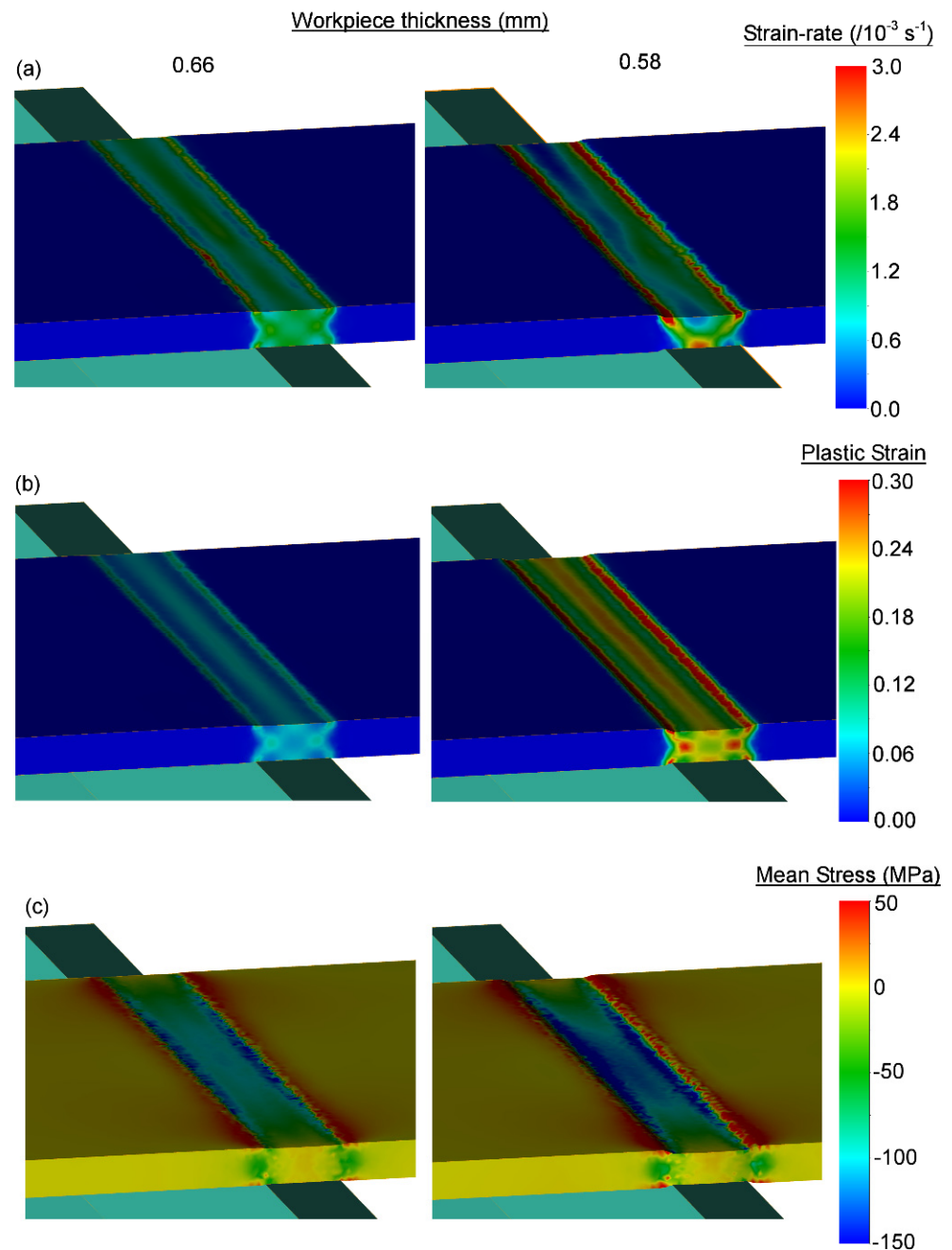


Figure 5. Distribution of (a) strain-rate, (b) plastic strain, and (c) mean stress at different stages of plane strain compression considering 3D conditions.

In order to estimate the accuracy of the plane strain compression test to determine the stress–strain behavior of the material, the load and displacement data from the 3D simulations were converted to effective stress and effective strain considering the relationships in Equations (2) and (3). Figure 6 shows the simulated stress–strain curves for simulations considering frictionless conditions and the simulation considering a friction coefficient of 0.15. The theoretical curve, used as input in the simulations, is also shown for comparison. The simulated curves display a minor fluctuation which is attributed to the oscillations in the deformation zone. In fact, experiments revealed some fluctuations in the response of

the PSC test, which tend to overestimate the flow stress depending on the b/t ratio [11]. This agrees with the slight overestimation of the flow stress in the stress–strain curves from the simulations. Another source of deviation in the stress–strain curve is the heterogeneity of distribution of plastic deformation which tends to concentrate deformation and therefore promotes a faster local strain-hardening. This effect is only expected in materials which display strain-hardening behavior. Therefore, it is anticipated that the accuracy of the test is better in samples processed by severe plastic deformation which usually does not display hardening.

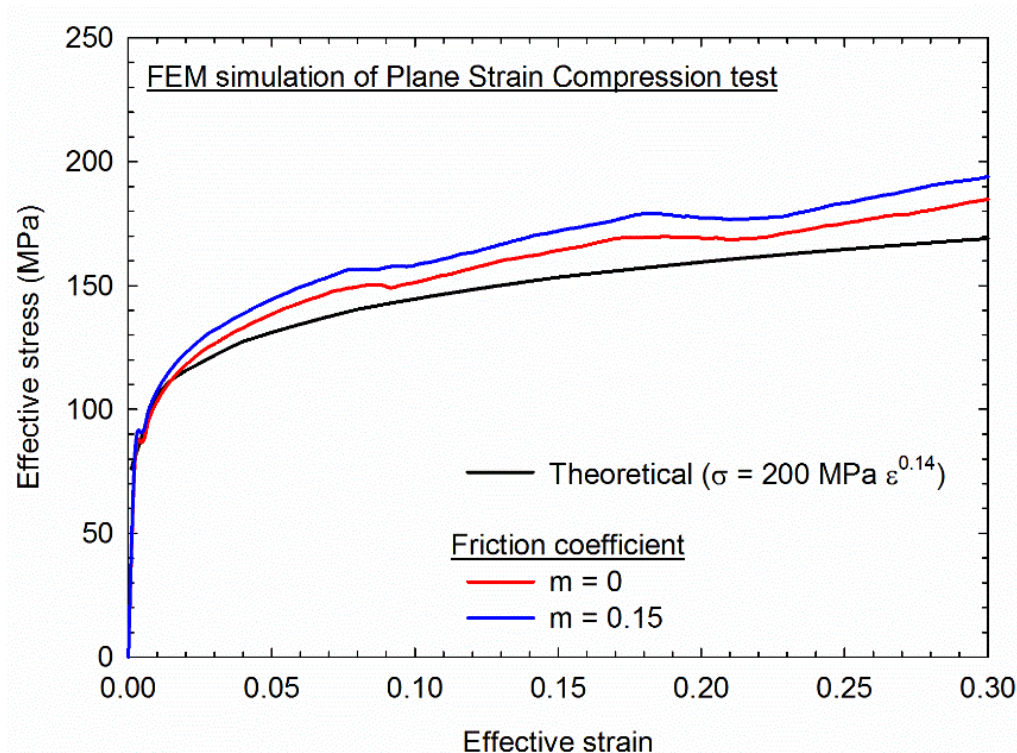


Figure 6. Stress vs. strain curves obtained from the PSC simulations considering different friction conditions, the theoretical input curve is also shown for comparison.

The friction between tool and workpiece promotes an increase in the load during compression which affects the stress–strain prediction. This effect is limited to less than 7% for a friction coefficient of 0.15. In spite of these effects, the simulated curves show excellent agreement with the theoretical curve at the beginning of the test. Therefore, it is expected that the PSC test provides accurate estimates of the yield stress.

3.2. PSC Tests in Magnesium

Figure 7a shows stress–strain curves obtained from tests in pure magnesium in the hot-rolled (initial) condition and after 1/8 turn and 2 turns of HPT. These numbers of turns were chosen based on a previous study which showed that 1/8 turn provides partial refinement of the grain structure of pure magnesium and 2 turns introduce the finest grain size of $\sim 0.6 \mu\text{m}$ and highest ductility [19]. The hot-rolled material displays a peak stress of $\sim 180 \text{ MPa}$ immediately after yielding and a decrease in flow stress which is attributed to the propagation of a crack. This level of flow stress is in the range of the ultimate tensile strength of $\sim 170 \text{ MPa}$ reported in a similar material with similar processing [20]. A peak flow stress of $\sim 180 \text{ MPa}$ was also observed during conventional compression perpendicular to the rolling plane in a similar material although the amount of strain from yielding to peak stress differs from the PSC result [21]. The material processed to 1/8 of a turn in HPT displays an enhanced strength with a peak flow stress of $\sim 220 \text{ MPa}$ and improved ductility compared to the rolled condition. Further processing to 2 turns of HPT reduced

the strength and increased significantly the ductility of pure magnesium. Both trends agree with results from tensile tests in a similar material [19].

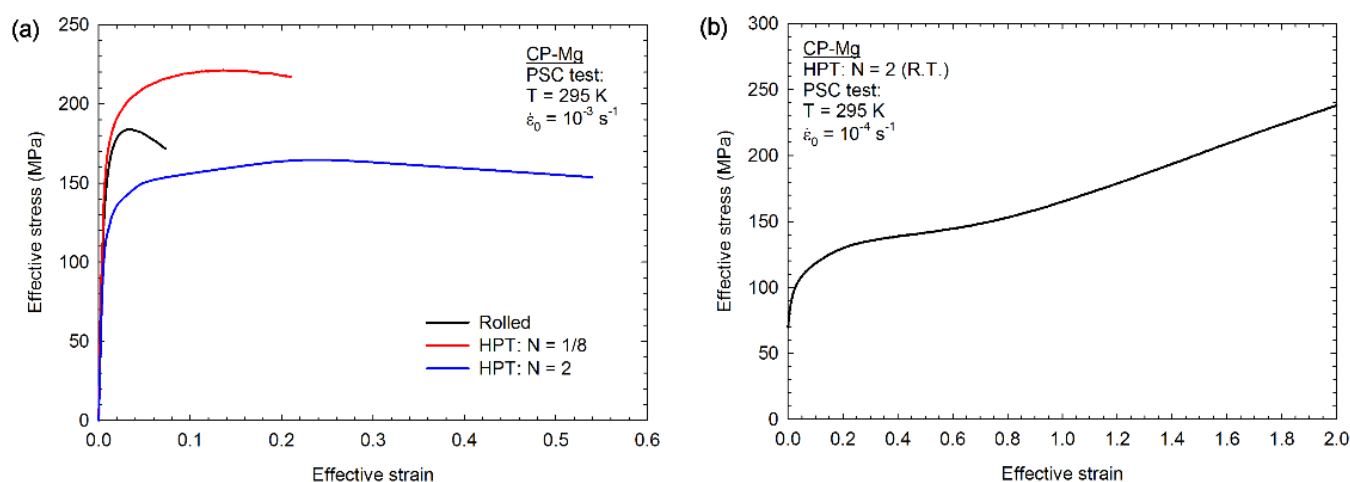


Figure 7. Stress vs. strain curves for pure magnesium determined in PSC tests at initial strain rates of (a) 10^{-3} s^{-1} and (b) 10^{-4} s^{-1} .

It is now well-known that HPT processing introduces exceptional ductility in pure magnesium and this effect is more obvious at lower strain rates [22]. Thus, an additional test was carried out at a lower strain-rate in the material processed to 2 turns of HPT and the curve is shown in Figure 7b. The flow stress level and the shape of the curve up to a strain of ~ 0.2 agree with the reported data for conventional compression perpendicular to the disc plane in pure magnesium processed by HPT [21]. The flow stress does not decrease at any level of strain and no visible cracks developed in this material up to strains larger than ~ 2 which is associated with a workpiece thickness of $\sim 100 \mu\text{m}$. This demonstrates the exceptional ductility introduced by HPT in this material. It is important to note that the stress strain curve displays a curvature upward at strains larger than ~ 0.6 and this is attributed to friction effects that play a major role on the load in PSC tests at large b/t ratios.

Plane strain compression tests were also carried out in the magnesium alloy AZ31. Figure 8 shows the stress–strain curves for samples in the extruded condition and after HPT processing to 1 and 10 turns. The largest number of turns was chosen based on a previous study which showed this processing condition leads to an ultrafine grain structure with average grain size of $\sim 130 \text{ nm}$ [23]. The extruded material displays a low yield stress of $\sim 75 \text{ MPa}$ followed by a pronounced strain hardening up to a peak stress of $\sim 360 \text{ MPa}$ at ~ 0.12 strain. The level of yield stress, peak stress, and the shape of the curve agrees fairly well with conventional compression of extruded AZ31 alloy with a coarse-grained structure [24]. The material processed by HPT displays significantly higher yield stress and reduced ductility. The peak stress in the material processed by 10 turns of HPT was $\sim 385 \text{ MPa}$. This peak stress agrees fairly well with the range of hardness ($105\text{--}125 \text{ kgf/mm}^2$) reported in the literature [23,25–27] for this alloy after HPT processing considering that the flow stress is approximately $1/3$ of the hardness [28]. Crack propagation was observed in all samples after the peak stress.

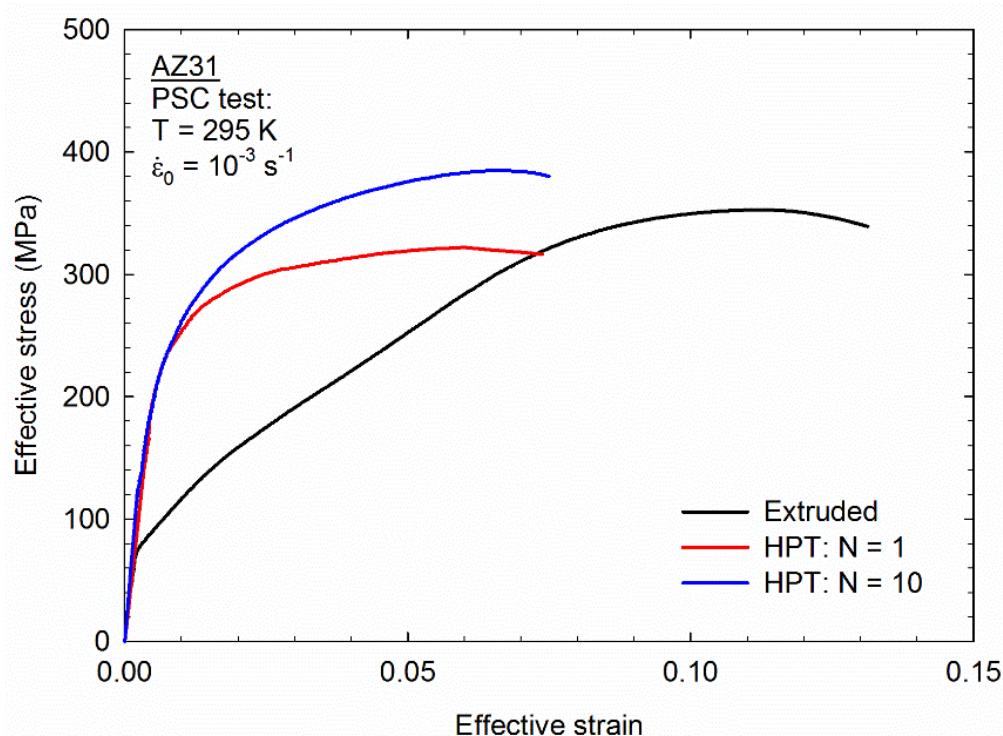


Figure 8. Stress vs. strain curves for AZ31 magnesium alloy with different processing conditions.

4. Discussion

Plane strain compression testing presents a great potential to evaluate the mechanical behavior of thin samples which are common in laboratory scale processes such as high-pressure torsion. The present study shows that it is possible to design an appropriate tool for testing samples with typical dimensions of discs produced by HPT without compromising the important geometric relations of larger tools. The finite element analysis shows that the shape of the deformation zone varies during deformation and this agrees with early predictions [29]. It also shows that deformation takes place under compressive mean stresses.

The finite element analysis also evaluated the accuracy of the output of testing in comparison with the input stress strain behavior. Deviations from the input stress strain curves were observed and attributed to the heterogeneity of distribution of strain and friction between the tool and the workpiece. These deviations are expected to decrease in materials with low strain-hardening ability and in well-lubricated tests. It is possible to subtract the contribution from friction by the use of a different equation for the estimation of the effective stress or by carrying out tests in samples of different initial thickness of a similar material [10]. It is also possible to take the inhomogeneity of deformation into account when treating data [30]. It is important to bear in mind that the present FEM analysis considered isotropic behavior of the workpiece and did not consider strain-rate sensitivity effects. Thus, further deviations may take place when testing anisotropic materials and materials with significant strain rate sensitivity. In practice, the output from the PSC test is not expected to be less accurate than microhardness tests or tensile tests in miniature samples in which the length to cross-sectional area and the displacement data acquisition are not adequate.

The present study also showed that a custom-designed PSC tool can be used to evaluate the mechanical behavior of pure magnesium and a magnesium alloy after processing by HPT. These two materials display distinct behavior since the former becomes extremely ductile after HPT processing and the later becomes brittle. The results show that the PSC test output agrees fairly well with data from the literature for tensile, compression, and microhardness testing of these materials. It is important to note that magnesium alloys tend

to display brittle behavior after HPT processing. There are reports of stress–strain curves from tensile tests of miniature samples of ZK60 [7] and ZKX600 [8] processed by HPT which displays failure without any significant plastic deformation. Previous attempts (not shown here) in our research group to carry out tensile tests on miniature samples of AZ31 alloy processed by HPT resulted in failure at low stress levels without noticeable yielding. Therefore, it is a major advance to be able to evaluate the flow stress in this material after HPT processing to multiple turns.

Although there is a report of plane strain compression experiments to evaluate the stress–strain behavior of metals over 70 year ago [9] this mechanical test has rarely been considered in research experiments in recent years. The present results show that PSC has great potential to aid in research, especially for the study of samples produced through laboratory-scale processing routes.

It is important to note that the amount of strain introduced during high pressure torsion processing varies along the sample radius. This inhomogeneity in strain distribution is expected to affect microstructure development and mechanical properties. The plane strain compression test evaluates the mechanical behavior of a large volume of the specimen and therefore it provides an average response of the material. The difference in mechanical behavior is expected to decrease and the accuracy of the PSC test increases with increasing the numbers of rotations in materials that display saturation in microstructure evolution.

5. Summary and Conclusions

A tool for plane strain compression (PSC) of thin samples produced by high-pressure torsion (HPT) was designed and constructed. Finite element modeling was used to estimate distribution of stress and strain and the accuracy in predicting the stress–strain behavior. The test is used to evaluate the mechanical response of pure magnesium and a magnesium alloy processed by HPT.

Finite element modeling reveals that the deformation zone is not homogeneous and its shape varies during plane strain compression. The distribution of strain is slightly heterogeneous.

The predicted stress–strain curve tends to overestimate the level of stresses by a few percent. This is attributed to the geometry of the deformation zone, strain localization during the test and friction effects.

Plane strain compression of pure magnesium revealed the expected softening and increase in ductility after multiple turns of HPT. This test was able to impose a few percent plastic deformation and estimate the flow stress in a magnesium alloy AZ31 processed by HPT. This is an advance by comparison with the brittle behavior observed during tensile tests of this material.

Despite the slight difference between the theoretical stress–strain curve and the curve obtained from finite element modeling, the PSC test is an effective way to evaluate mechanical behavior of the small samples produced by HPT.

Author Contributions: Conceptualization, R.P.R.P.P., P.H.R.P., R.B.F.; methodology, A.P.C., L.M.R., R.B.F., validation, A.P.C., L.M.R.; writing—review and editing, A.P.C., L.M.R., R.P.R.P.P., P.H.R.P., T.G.L., R.B.F. All authors have read and agreed to the published version of the manuscript.

Funding: P.H.R.P. acknowledges financial support from CNPq (grant 443736/2018-9) and FAPEMIG (grant APQ-01342-21). T.G.L. acknowledges financial support from ERC (grant 267464-SPDMETALS). R.B.F. acknowledges financial support from CNPq (grant 302445/2018-8) and FAPEMIG (grant TEC-PPM-00324-17).

Data Availability Statement: The data that support the findings of this study are available from the corresponding author, upon reasonable request.

Conflicts of Interest: The authors declare no conflict of interest.

References

1. Zhilyaev, A.P.; Langdon, T.G. Using high-pressure torsion for metal processing: Fundamentals and applications. *Prog. Mater. Sci.* **2008**, *53*, 893–979. [\[CrossRef\]](#)
2. Hohenwarter, A.; Bachmaier, A.; Gludovatz, B.; Scheriau, S.; Pippan, R. Technical parameters affecting grain refinement by high pressure torsion. *Int. J. Mater. Res.* **2009**, *100*, 1653–1661. [\[CrossRef\]](#)
3. Hohenwarter, A.; Pippan, R. Sample Size and Strain-Rate-Sensitivity Effects on the Homogeneity of High-Pressure Torsion Deformed Disks. *Metall. Mater. Trans. A* **2019**, *50*, 601–608. [\[CrossRef\]](#)
4. Figueiredo, R.B.; De Faria, G.C.V.; Cetlin, P.R.; Langdon, T.G. Three-dimensional analysis of plastic flow during high-pressure torsion. *J. Mater. Sci.* **2013**, *48*, 4524–4532. [\[CrossRef\]](#)
5. Rathmayr, G.B.; Bachmaier, A.; Pippan, R. Development of a new testing procedure for performing tensile tests on specimens with sub-millimetre dimensions. *J. Test. Eval.* **2013**, *41*. [\[CrossRef\]](#)
6. Figueiredo, R.B.; Langdon, T.G. Deformation mechanisms in ultrafine-grained metals with an emphasis on the Hall-Petch relationship and strain rate sensitivity. *J. Mater. Res. Technol.* **2021**, *14*, 137–159. [\[CrossRef\]](#)
7. Torbati-Sarraf, S.A.; Sabbaghianrad, S.; Langdon, T.G. Using Post-Deformation Annealing to Optimize the Properties of a ZK60 Magnesium Alloy Processed by High-Pressure Torsion. *Adv. Eng. Mater.* **2018**, *20*, 1700703. [\[CrossRef\]](#)
8. Zheng, R.X.; Bhattacharjee, T.; Shibata, A.; Sasaki, T.; Hono, K.; Joshi, M.; Tsuji, N. Simultaneously enhanced strength and ductility of Mg-Zn-Zr-Ca alloy with fully recrystallized ultrafine grained structures. *Scr. Mater.* **2017**, *131*, 1–5. [\[CrossRef\]](#)
9. Ford, H. Researches into the Deformation of Metals by Cold Rolling. *Proc. Inst. Mech. Eng.* **1948**, *159*, 115–143. [\[CrossRef\]](#)
10. Mohebbi, M.S.; Akbarzadeh, A.; Yoon, Y.-O.; Kim, S.-K. Flow stress analysis of ultrafine grained AA 1050 by plane strain compression test. *Mater. Sci. Eng. A* **2014**, *593*, 136–144. [\[CrossRef\]](#)
11. Watts, A.B.; Ford, H. An Experimental Investigation of the Yielding of Strip between Smooth Dies. *Proc. Inst. Mech. Eng.* **1953**, *167*, 448–464. [\[CrossRef\]](#)
12. QForm 10.1.3. Available online: <https://www.qform3d.com/> (accessed on 16 December 2021).
13. Figueiredo, R.B.; Cetlin, P.R.; Langdon, T.G. Using finite element modeling to examine the flow processes in quasi-constrained high-pressure torsion. *Mater. Sci. Eng. A* **2011**, *528*, 8198–8204. [\[CrossRef\]](#)
14. Figueiredo, R.B.; Pereira, P.H.R.; Aguilar, M.T.P.; Cetlin, P.R.; Langdon, T.G. Using finite element modeling to examine the temperature distribution in quasi-constrained high-pressure torsion. *Acta Mater.* **2012**, *60*, 3190–3198. [\[CrossRef\]](#)
15. Dieter, G.E. *Mechanical Metallurgy*, 3rd ed.; McGraw-Hill Book Company: London, UK, 1988.
16. Sae-Eaw, N.; Aue-U-Lan, Y. Mechanical property determination for combined sheet and bulk metal forming process by plane strain compression test. *Mater. Today Proc.* **2018**, *5*, 9376–9383. [\[CrossRef\]](#)
17. Gelin, J.C.; Ghouati, O.; Shahani, R. Modelling the plane strain compression test to obtain constitutive equations of aluminium alloys. *Int. J. Mech. Sci.* **1994**, *36*, 773–796. [\[CrossRef\]](#)
18. Pietrzyk, M.; Lenard, J.G.; Dalton, G.M. A Study of the Plane Strain Compression Test. *CIRP Ann.* **1993**, *42*, 331–334. [\[CrossRef\]](#)
19. Figueiredo, R.B.; Pereira, P.H.R.; Langdon, T.G. Effect of Numbers of Turns of High-Pressure Torsion on the Development of Exceptional Ductility in Pure Magnesium. *Adv. Eng. Mater.* **2020**, *22*, 1900565. [\[CrossRef\]](#)
20. Silva, C.L.P.; Oliveira, A.C.; Costa, C.G.F.; Figueiredo, R.B.; de Fátima Leite, M.; Pereira, M.M.; Lins, V.F.C.; Langdon, T.G. Effect of severe plastic deformation on the biocompatibility and corrosion rate of pure magnesium. *J. Mater. Sci.* **2017**, *52*, 5992–6003. [\[CrossRef\]](#)
21. Silva, C.L.P.; Camara, M.A.; Hohenwarter, A.; Figueiredo, R.B. Mechanical Behavior and In Vitro Corrosion of Cubic Scaffolds of Pure Magnesium Processed by Severe Plastic Deformation. *Metals* **2021**, *11*, 1791. [\[CrossRef\]](#)
22. Figueiredo, R.B.; Sabbaghianrad, S.; Giwa, A.; Greer, J.R.; Langdon, T.G. Evidence for exceptional low temperature ductility in polycrystalline magnesium processed by severe plastic deformation. *Acta Mater.* **2017**, *122*, 322–331. [\[CrossRef\]](#)
23. Silva, C.L.P.; Soares, R.B.; Pereira, P.H.R.; Figueiredo, R.B.; Lins, V.F.C.; Langdon, T.G. The Effect of High-Pressure Torsion on Microstructure, Hardness and Corrosion Behavior for Pure Magnesium and Different Magnesium Alloys. *Adv. Eng. Mater.* **2019**, *21*, 1801081. [\[CrossRef\]](#)
24. Barnett, M.R.; Keshavarz, Z.; Beer, A.G.; Atwell, D. Influence of grain size on the compressive deformation of wrought Mg–3Al–1Zn. *Acta Mater.* **2004**, *52*, 5093–5103. [\[CrossRef\]](#)
25. Figueiredo, R.B.; Langdon, T.G. Processing Magnesium and Its Alloys by High-Pressure Torsion: An Overview. *Adv. Eng. Mater.* **2019**, *21*, 1801039. [\[CrossRef\]](#)
26. Straska, J.; Janecek, M.; Gubicza, J.; Krajnak, T.; Yoon, E.Y.; Kim, H.S. Evolution of microstructure and hardness in AZ31 alloy processed by high pressure torsion. *Mater. Sci. Eng. A* **2015**, *625*, 98–106. [\[CrossRef\]](#)
27. Huang, Y.; Figueiredo, R.B.; Baudin, T.; Brisset, F.; Langdon, T.G. Evolution of strength and homogeneity in a magnesium AZ31 alloy processed by high-pressure torsion at different temperatures. *Adv. Eng. Mater.* **2012**, *14*, 1018–1026. [\[CrossRef\]](#)
28. Tabor, D. A Simple Theory of Static and Dynamic Hardness. *Proc. R. Soc. Lond. Ser. A-Math. Phys. Sci.* **1948**, *192*, 247–274. [\[CrossRef\]](#)
29. Green, A.P. XCII. A theoretical investigation of the compression of a ductile material between smooth flat dies. *Lond. Edinb. Dublin Philos. Mag. J. Sci.* **1951**, *42*, 900–918. [\[CrossRef\]](#)
30. Kowalski, B.; Lacey, A.J.; Sellars, C.M. Correction of plane strain compression data for the effects of inhomogeneous deformation. *Mater. Sci. Technol.* **2003**, *19*, 1564–1570. [\[CrossRef\]](#)